NORWEGIAN JOURNAL OF GEOLOGY Vol 95 Nr. 2 (2015)
http://dx.doi.org/10.17850/njg95-2-04

GEOLOGICAL SOCIETY OF NORWAY

Variability of present and past PAH (polyaromatic hydrocarbons) concentrations in sediments of the SW Barents Sea

Juho Junttila[1], JoLynn Carroll[1,2,3] & Noortje Dijkstra[1]

[1]*Department of Geology, UiT The Arctic University of Norway, Dramsveien 201, 9037 Tromsø, Norway.*
[2]*Akvaplan-niva AS, FRAM - High North Research Centre for Climate and the Environment, 9296 Tromsø, Norway.*
[3]*CAGE — Centre for Arctic Gas Hydrate, Environment and Climate, UiT The Arctic University of Norway, 9037 Tromsø, Norway.*

E-mail corresponding author (Juho Junttila): juho.junttila@uit.no

The concentration and distribution of polyaromatic hydrocarbons (PAHs) in surface and subsurface sediment samples from Tromsøflaket and Ingøydjupet, southwestern Barents Sea, were investigated in order to provide insight into the levels and origins of PAHs in a region with petroleum activities. PAH profiles in sediments were evaluated in context with sediment grain size and total organic carbon in order to assess the influence of ocean currents on the transportation and deposition of PAHs. The PAH concentrations are of background (Level I) to good level (Level II) based on the Water Framework Directive classification system. SUM PAH (SUM of 26 PAH compounds) ranged from 39 to 2197 µg/kg (average 225 µg/kg), and NPD (naphthalene, phenanthrene and dibenzothiophene, including their C1–C3 alkyl homologues) in surface samples ranged from 14 to 2045 µg/kg (average 157 µg/kg). However, the average values presented here are higher than have been reported in previous studies. The observed changes in PAH contents in surface and subsurface sediments vary in accordance with changes in grain size (clay and silt 17–99%) and total organic carbon content (0.37–0.98%). In turn, these sedimentary parameters are controlled by the inflow of Atlantic Water and the strength of the two predominating current systems in this region: the North Atlantic Current and Norwegian Coastal Current. Source-allocation modeling suggests that PAHs in surface samples are mainly of pyrogenic or mixed pyrogenic and petrogenic origin. Taken together, these patterns of PAH levels and sources reflect natural variability, indicating that the derived dataset establishes a pre-impacted baseline of the present state of the seafloor.

Keywords: Barents Sea, hydrocarbons, baseline studies, marine geology, sediments, currents

Electronic Supplements 1–6

Received 23. February 2015 / Accepted 17. August 2015 / Published online 9. October 2015.

Introduction

Large hydrocarbon reserves have been identified in the Norwegian sector of the Barents Sea (Goliat, Skrugard and Havis). One of the waste streams associated with the seafloor extraction of these hydrocarbon resources is drill cuttings. Drill-cutting discharges consist of a mixture of man-made and natural substances containing higher concentrations of polyaromatic hydrocarbons (PAHs) and metals than observed in natural sediments. PAHs are especially important because of their persistence, ability to bioaccumulate, and toxicity (Neff, 2002; Boitsov et al., 2009a, b). Increasing petroleum activity in the Southwest Barents Sea will lead to an increase in releases of drill cuttings into the ocean. A baseline evaluation of sediment and contaminant transport and deposition processes is therefore needed to establish an effective strategy for the handling of these discharges.

In the present paper, we investigate the effect of ocean currents on the transportation of PAH-laden sediments in the Southwest Barents Sea (Fig. 1). PAHs are ubiquitous in nature. Generally, there are three major types of PAHs which may be found in freshwater and marine sediments depending on their genesis: biogenic, petrogenic,

Junttila, J., Carroll, J. & Dijkstra, N. 2015: Variability of present and past PAH concentrations in sediments of the SW Barents Sea. *Norwegian Journal of Geology 95*, 191–210. http://dx.doi.org/10.17850/njg95-2-04.

and pyrogenic. PAHs of biogenic origin are generated by biological processes or by the early stages of diagenesis in marine sediments (e.g., perylene) (Venkatesan, 1988). PAHs of petrogenic origin, formed by low- to moderate-temperature diagenesis of sediment organic matter to fossil fuels, are present in oil and some oil products. PAHs of pyrogenic origin are formed by incomplete combustion of organic material (e.g., Page et al., 1999). Sources of pyrogenic PAHs are forest fires and incomplete combustion of fossil fuels. In the coastal zone, PAHs enter the water primarily from sewage, runoff from roads, the smelter industry and oil spills (e.g., Dalsøren et al., 2007). Generally, in the marine environment, PAHs may enter the water through oil seeps, oil spills, and produced water discharge from offshore oil installations.

The geographic focus of the present investigation is the shallow bank of Tromsøflaket, the deeper trough of Ingøydjupet and the southern part of the trough of Bjørnøyrenna (Fig. 1). Ingøydjupet has been formed by an eroding ice sheet, leaving Tromsøflaket at a higher elevation on the west side, whereas Nordkappbanken has been formed mainly by sediments deposited in front of an ice sheet (Andreassen et al., 2008). Erosion by a major ice stream is also responsible for the formation of the Bjørnøyrenna trough from which large amounts of sediments were delivered to the Bjørnøya trough mouth fan during the last glacial maximum (Andreassen et al., 2008). In general, coarse-grained sediments are observed in shallow depths due to strong bottom currents. Finer material deposits are observed at greater depths due to weak ocean currents (Bellec et al., 2008 and references therein; Dijkstra et al., 2013; Junttila et al., 2014).

The seafloor sedimentary environment in the Southwest Barents Sea is generally influenced by strong currents on the shallow banks, Tromsøflaket and Nordkappbanken, and low-energy currents in the deeper depressions of Ingøydjupet (Fig. 1; Bellec et al., 2008; Jensen et al., 2009; Junttila et al., 2014). The main ocean currents in the Southwest Barents Sea are the Norwegian Coastal Current (NCC) and the North Atlantic Current (NAC) (Fig. 1). The NCC is a shallow surface current, which follows the Norwegian coast towards the north (Mosby, 1968; Ersdal, 2001; Ingvaldsen et al., 2004; Asplin et al., 2006). The NCC dominates with several, relatively permanent, small and large eddies present at the shallow Tromsøflaket (Fig. 1; Bjerke & Torsethaugen, 1989). The NAC is a deep-water current that transports material along the continental shelf northwards (Gjevik, 2000; Bellec et al., 2008). This current turns toward Bjørnøyrenna and also extends into shallower water depths at Tromsøflaket due to the prevailing southwesterly winds (Ingvaldsen et al., 2004).

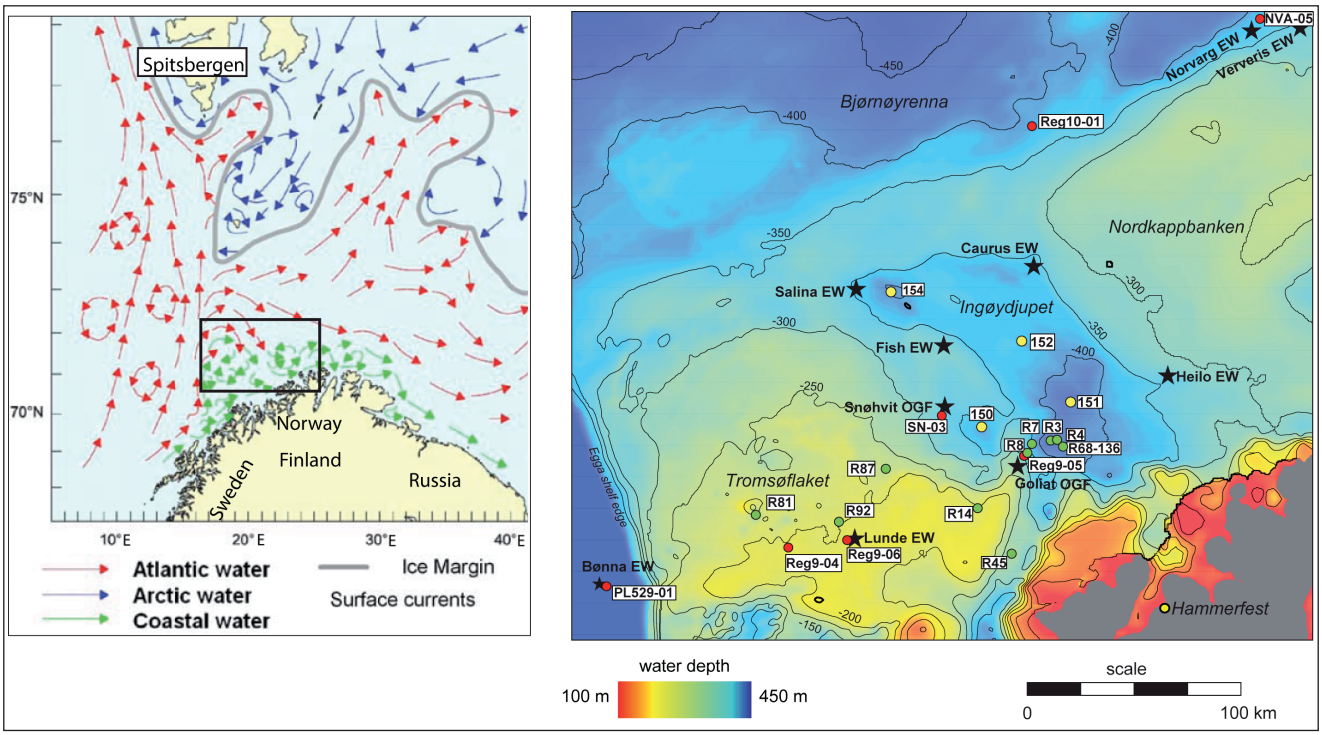

Figure 1. *The left panel shows the major ocean currents and the average location of the sea-ice margin in the southwestern Barents Sea (Sakshaug & Skjoldal, 1989) with the study area marked by a rectangle. The right panel provides a detailed bathymetric map of the study area. The yellow color indicates shallow water depths and the blue color deep-water depths. Also shown are the surface sample stations (green circles from Mareano, red circles from Statoil) and multicore stations (yellow circles). Petroleum exploration well (EW) sites and the Goliat and Snøhvit oil and gas fields (OGF) are indicated by stars.*

Since 1998, environmental monitoring of the Southwest Barents Sea has been carried out as part of the Norwegian offshore monitoring program for the petroleum sector (Iversen et al., 2011) The focus of these surveys is benthic biodiversity, sediment characterization and chemical composition (Bakke et al., 2001; Trannum et al., 2004; Mannvik & Wasbotten, 2008; Nøland et al., 2009; Mannvik et al., 2011). A number of studies on the environment of the Southwest Barents Sea carried out through the MAREANO project have shown that PAH and heavy-metal levels are at background levels indicating natural conditions in bottom sediments (Boitsov et al., 2009a, b; Jensen et al., 2009; Knies & Martinez, 2009; Vogt & Knies, 2009). Baseline levels and sources of PAH in the Barents Sea have also been investigated in the past (Dahle et al., 2006, 2009; Boitsov et al., 2009a, b, 2011, 2013). These studies also found background levels of PAHs.

PAH deposition is due to a complex sedimentation regime controlled by ocean water mass transport and mixing with coastal discharges, coastal abrasion, and atmospheric transport. Bottom current transportation of fine-grained sediments and heavy-metal concentrations based on the same sample material as presented in this paper has been studied previously (Dijkstra et al., 2013, 2015; Junttila et al., 2014). Through these earlier studies, there is a clear connection between bottom current strength, fine particle deposition, and heavy-metal concentrations. This relationship depends mainly on water depth and the influence of the two main currents in the Southwest Barents Sea: the NAC and the NCC. However, the effect of these ocean currents on the transportation of PAH concentrations has not been studied in detail.

Here, we perform a baseline study of PAHs and report on the concentration and distribution of PAHs in surface and subsurface sediment samples from Tromsøflaket and Ingøydjupet. These results are evaluated in context with sedimentary properties, namely, sediment grain size (sand, silt, clay) and Total Organic Carbon (TOC) content. By using these proxies, this study provides additional insight into the influence of ocean currents on the transportation and deposition of PAHs in a region where petroleum activities are currently undergoing an expansion.

Methods

Sample stations

The sample material is divided into a set of surface samples, covering the top cm (0–1 cm) of the sediment surface, and multicore samples from 0–20 cm depth, subsampled at 1 cm intervals. Sample information is presented in Table 1. Ten surface samples were collected in 2006 and 2007 (MAREANO set) (see Jensen et al., 2007, 2008; Dijkstra et al., 2013). In addition, 7 samples were collected in the summer of 2010 (Statoil set). These were collected as part of the Norwegian offshore monitoring program and it is required by the operator (Statoil) to take three replicate samples at each site (see Mannvik et al., 2011). In the summer of 2011, multicore samples were collected from different locations in Ingøydjupet (University of Tromsø (UiT) set), as described in Junttila et al. (2014) and Dijkstra et al. (2015).

All of the samples were analyzed for grain size, TOC, PAH compounds, and ^{210}Pb dating (for sediment age determinations).The grain-size and TOC data for the surface samples have been previously published in Dijkstra et al. (2013) and the grain size, TOC data, and ^{210}Pb dating for the sediments cores have been previously published in Junttila et al. (2014). The PAH compositions for the Statoil set have been previously published in Mannvik et al. (2011). It should also be noted that the PAH compounds could not be analyzed on the top 1 cm of the cores 152 and 154 since there was not enough material. In Fig. 2, samples from 2 cm depth have been used for these cores.

Grain sizes

All samples were sieved (>1 mm, >100 μm, >63 μm) to perform grain-size analyses on the coarse fraction and to collect foraminifera for further studies (Dijkstra et al., 2013, 2015). Smaller fractions (<63 μm) were further analyzed by using the sedigraph technique (Coakley & Syvitski, 1991). The sortable silt mean grain size ($\overline{SS}$) was calculated from the 10–63 μm fraction. For more detailed descriptions of these methods, see Junttila et al. (2014) and Dijkstra et al. (2013).

Age model and sediment accumulation rates

The subsurface sediment cores were dated using unsupported ^{210}Pb dating. Ages used to interpret the down core sedimentary PAH profiles in the present paper were determined by the Constant Rate of Supply model (CRS). For a more detailed description of this method, see Junttila et al. (2014).

TOC

The TOC concentrations of the samples of the MAREANO and UiT-set were analyzed using a Leco CS–200 induction furnace at the Geological Survey of Norway (NGU) and UiT, respectively (Table 1; see Dijkstra et al. (2013) and Junttila et al. (2014)). TOC was obtained by HCl extraction of crushed sample material assuming that the dissolved material was calcium carbonate ($CaCO_3$), and thereafter combusted in the Leco furnace at 1350°C.

Table 1. *Sample station locations, type and place of analyses, and water depth.*

Sample	***Location***		***Analyses***			***Water depth***
MAREANO 2006	*Lat.*	*Long.*	*Grain size*	*TOC*	*PAH*	*(m)*
R3	71.34	22.43	BC(UiT)		MC(UL)	435
R4	71.34	22.49	BC(UiT)		MC(UL)	433
R7	71.33	22.21	BC(UiT)		MC(UL)	355
R8	71.28	22.14	BC(UiT)		MC(UL)	313
R14	71.13	21.44	BC(UiT)		MC(UL)	221
R45	70.89	21.80	GC(UiT)		N/A	300
R68-136	71.32	22.49	BC(UiT)		MC(UL)	440
MAREANO 2007						
R81	71.16	18.65	BC(UiT)		MC(UL)	349
R87	71.30	20.34	BC(UiT)		MC(UL)	239
R92	71.07	19.57	BC(UiT)		N/A	202
Statoil 2010						
NVA-05*	72.92	25.89	GC(UiT)		GC(UL)	381
PL529*	70.85	16.56	BC(UiT)		BC(UL)	1389
reg 09-04*	71.00	19.00	GC(UiT)		GC(UL)	187
reg 09-05*	71.28	22.12	GC(UiT)		GC(UL)	307
reg 09-06*	71.03	19.66	GC(UiT)		GC(UL)	194
reg 10-01*	72.63	22.78	GC(UiT)		GC(UL)	382
SN-03*	71.49	21.09	GC(UiT)		GC(UL)	326
UiT 2011						
HH-11-150 MC	71.41	21.64	MC(UiT)	MC(UiT)	MC(UL)	383
HH-11-151 MC	71.50	22.77	MC(UiT)	MC(UiT)	MC(UL)	434
HH-11-152 MC	71.74	22.32	MC(UiT)	MC(UiT)	MC(UL)	394
HH-11-154 MC	72.02	20.60	MC(UiT)	MC(UiT)	MC(UL)	400

*Sample stations are divided into 3 replicates, except PL529, which is divided into 2 replicates.
UiT: University of Tromsø; UL: UniLab; MC: Multicore; GC:Grabcore; BC: Boxcore.

Sample preparation and PAH analysis

Individual sediment samples were homogenized, treated with methanol and potassium hydroxide (KOH), and refluxed for 1.5 hours together with a 1.0 ml solution of 7 deuterated PAHs (Dahle et al., 2009). The solid fraction was removed by filtration and the eluant containing PAHs was extracted with pentane. The extracts were purified by column chromatography using Varian Bond Elute solid phase extraction cartridges containing 500 mg silica (Varian LRC, A1211–3036) and eluted with pentane and dichloromethane. The final extract was analyzed by capillary column gas chromatography with mass spectrometric detection (Hewlett-Packard MS 5971, HP 5890 Gas Chromatograph equipped with a split/splitless injector and a 25 m x 0.20 mm ID HP Ultra 1 column, and HP G 1034 B software for MS ChemStation). In accordance with the Norwegian offshore monitoring program, the analysis of 16 EPA–PAH compounds (Statoil set) was carried out at the commercial laboratory, Unilab analyse AS, as presented in Mannvik et al. (2011). Unilab analyse AS is accredited for hydrocarbon analyses according to the European standards of NS–EN 45001 and ISO/IEC Guide 25.

Standard extraction procedure

Hydrocarbons were extracted from the sediment by boiling in potassium hydroxide in methanol followed by liquid-liquid extraction with organic solvent. The hydrocarbon fraction was then concentrated and isolated with Absorption Chromatography in a silica column (Mannvik et al., 2011).

Quantifying NPD and 16 EPA–PAH compounds

The content of naphthalene, phenanthrene and dibenzothiophene, including their C1–C3 alkyl homologues (NPD), PAH compounds (16 EPA–PAH) and decalins, were determined with a Gas-Chromatography mass-spectrometer and quantified with the help of deuterized internal standards. Limits of quantification (LOQ) for PAH–NPD were 0.013–3.3 µg/kg (average: 2.2 µg/kg) dry weight for individual parameters where the LOQ for 16 EPA–PAH were 0.05–1.4 µg/kg (average 0.56 µg/kg).

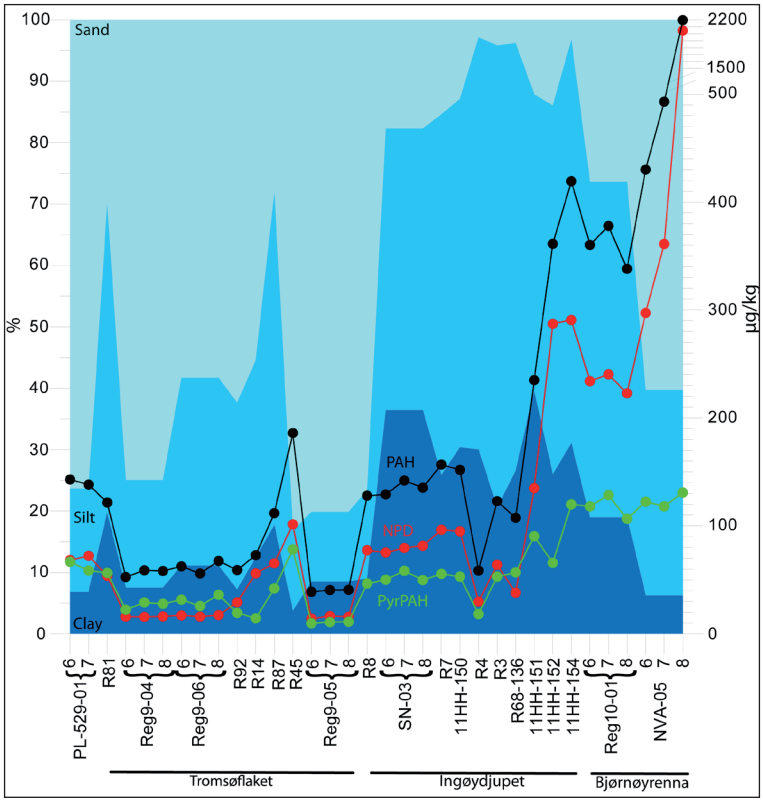

Figure 2. Clay, silt and sand are plotted cumulatively with different blue colors. The black, green, and red lines indicate SUM PAH, PyrPAH and NPD, respectively, in the different surface sample stations.

PAH sources

The approximate percentage of fossil PAHs relative to total PAHs is assessed by the Fossil Fuel Pollution Index (FFPI) (Boehm & Farrington, 1984):

$$FFPI = \left[\frac{N_s+P_s-1/2(P+C_1P)+D_s}{\sum PAH}\right] \times 100\%$$

where N_s is the sum of naphthalene and its alkyl homologues; P_s is the sum of phenanthrene and its alkyl homologues; P is the phenathrene concentrations; C_1P is methyl phenanthrene; D_s is the sum of dibenzothiophene and its alkyl homologues; ΣPAH is the total PAH concentration (sum of the two- to six-ring PAHs (26 compounds)).

The identification of PAH sources relies on so-called PAH 'fingerprints', that are diagnostic of the source and are based on the concentrations of individual PAH compounds (Page et al., 1999). Contributions of the possible source to PAH concentrations found in sediment samples were evaluated using a nonlinear estimation of source-allocation models. These models find the linear combination of sources that best represents the measured PAH profiles in a given sediment sample (Burns et al., 1997).

The goal of nonlinear estimation is to minimize a loss function, which is defined as the sum of the squared deviation about the predicted values: Σ (Observed value – Predicted value)^2.

$$\sum_{i=1}^{k}\left[\sum_{j=1}^{n}(s_{i,j}x_j|\Sigma PAH_j)-d_s|\Sigma PAH_{sample}\right]^2$$

where k is the number of the PAH compounds analyzed; n is the number of the tested possible PAH sources; $s_{i,j}$ is the concentration of its PAH compound in the PAH source; x_j is the fraction of the total PAH concentrations in the sample that is due to the PAH source; ΣPAH_j is the total PAH concentration of the PAH source; d_i is the concentration of the sample PAH compounds; ΣPAH_{sample} is the total PAH concentration in the sample. The computational procedure used to minimize the loss function recognizes that $0 < xj < 1$ and $\sum_{j=1}^{k} x_j = 1$ (Burns et al., 1997).

Literature data on individual analyses of possible PAH sources (crude oil, diesel oil, lightly weathered diesel oil, diesel soot, wood combustion soot, atmospheric dust NIST SRM 1649) (Burns et al., 1997; Page et al., 1999) , weathered creosote (Neff et al., 2005) and Svalbard's coal (Killie et al., 1997; Bjoroy et al., 2010) were used as diagnostic tools for identifying sources. Before performing the calculations the following data transformations were made: if CPAHi < MDL then CPAHi = 0.

Results

Surface samples

All sediment weights are reported as dry weight. Our measured surface sample concentrations for SUM PAH (SUM of all PAH) range from 39 to 2197 µg/kg (average 225 µg/kg). For NPD (Sum of naphthalene, dibenzothiophene, phenanthrene and their C1–C3 alkylated homologues), concentrations range from 14 to 2045 µg/kg (average 157 µg/kg), and for pyrogenic PAH (PyrPAH; sum of all the four- to six-ring PAH except perylene (Boitsov et al., 2009a) concentrations are 10–131 µg/kg (average 58 µg/kg) (Fig. 2; Table 2). SUM PAH is highest in surface samples mainly in the two northernmost stations, Reg–10–01 and NVA–05. The highest NPD and PyrPAH values are observed also in samples from the northernmost stations (Reg–10–01, NVA–05) and station 154 (Fig. 1). PyrPAH is higher than NPD at only three stations; Reg9–04, Reg9–06 and R68. Further, PyrPAH and NPD concentrations are similar at stations PL–529, R92, Reg9–05, R4 and R3, NPD and PyrPAH . Individual PAH results are given in Electronic Supplement 1 and Fig. 3.

Table 2. *FFPI values and selected PAH ratios in surface sediment samples.*

Sample	*Location*	*FFPI*	*Water depth (m)*	*Source allocation model*	*SUM PAH µg/kg*	*PyrPAH µg/kg*	*NPD µg/kg*
PL529-01-6	Continental rise	43.5	1389	Mixed	142.92	66.74	68.28
PL529-01-7		47.7	1389	Mixed	138.25	58.62	72.24
R81	Tromsøflak.	38.6	349	Pyrogenic	121.59	56.31	53.74
reg9-04-6	Tromsøflak.	6.3	187	Pyrogenic	52.59	22.33	15.84
reg9-04-7	Tromsøflak.	4.8	187	Pyrogenic	58.82	29.02	15.66
reg9-04-8	Tromsøflak.	5.6	187	Pyrogenic	58.21	27.77	16.08
reg9-06-6	Tromsøflak.	9.1	194	Pyrogenic	62.47	31.62	17.07
reg9-06-7	Tromsøflak.	6	194	Pyrogenic	55.79	25.73	15.88
reg9-06-8	Tromsøflak.	8.2	194	Pyrogenic	67.52	36.17	17.29
R92	Tromsøflak.	44.9	202	Mixed	59.08	19.34	29.17
R14	Tromsøflak.	75.1	221	Petrogenic	72.84	14.35	55.93
R87	Tromsøflak.	55	239	Mixed	111.73	41.96	65.31
R45	Ingøydjup.	49.3	300	Mixed	185.98	78.19	101.42
reg9-05-6	Ingøydjup.	n.d.	307	Pyrogenic	38.91	9.74	13.91
reg9-05-7	Ingøydjup.	21	307	Pyrogenic	40.49	10.79	16.43
reg9-05-8	Ingøydjup.	20.3	307	Pyrogenic	40.69	11.16	15.77
R8	Ingøydjup.	56.2	313	Mixed	127.90	46.56	77.37
SN-03-6	Ingøydjup.	53.1	326	Mixed	129.09	50.10	75.29
SN-03-7	Ingøydjup.	51	326	Mixed	141.95	58.38	79.53
SN-03-8	Ingøydjup.	54.9	326	Mixed	135.33	49.77	81.52
R7	Ingøydjup.	57.2	355	Mixed	156.69	55.46	96.35
11HH-150	Ingøydjup.	58.3	383	-	151.87	52.96	95.65
R4	Ingøydjup.	45.7	433	Mixed	58.57	18.25	29.80
R3	Ingøydjup.	46.5	435	Mixed	122.86	52.96	63.93
R68A-136	Ingøydjup.	28.2	440	Pyrogenic	107.43	56.90	38.06
11HH-151	Ingøydjup.	51.9	434	-	234.54	90.39	135.37
11HH-152	Ingøydjup.	73.2	394	-	361.30	65.75	287.86
11HH-154	Ingøydjup.	63.7	400	-	418.84	119.87	291.37
reg10-01-6	Bjørnøyr.	58.7	382	Mixed	360.27	118.04	233.99
reg10-01-7	Bjørnøyr.	57.4	382	Mixed	377.79	128.42	240.35
reg10-01-8	Bjørnøyr.	60.2	382	Mixed	338.13	106.47	222.80
NVA-05-6	Bjørnøyr.	63.4	381	Petrogenic	430.00	122.37	297.24
NVA-05-7	Bjørnøyr.	67.2	381	Petrogenic	492.87	118.06	361.15
NVA-05-8	Bjørnøyr.	89	381	Petrogenic	2197.09	130.82	2045.52
Average		44.58			225.01	58.27	157.15
Average*		39.83			123.37	44.90	69.36

Average* – average without reg10 and NVA.
Abbreviation: n.d. – not enough data for calculation.

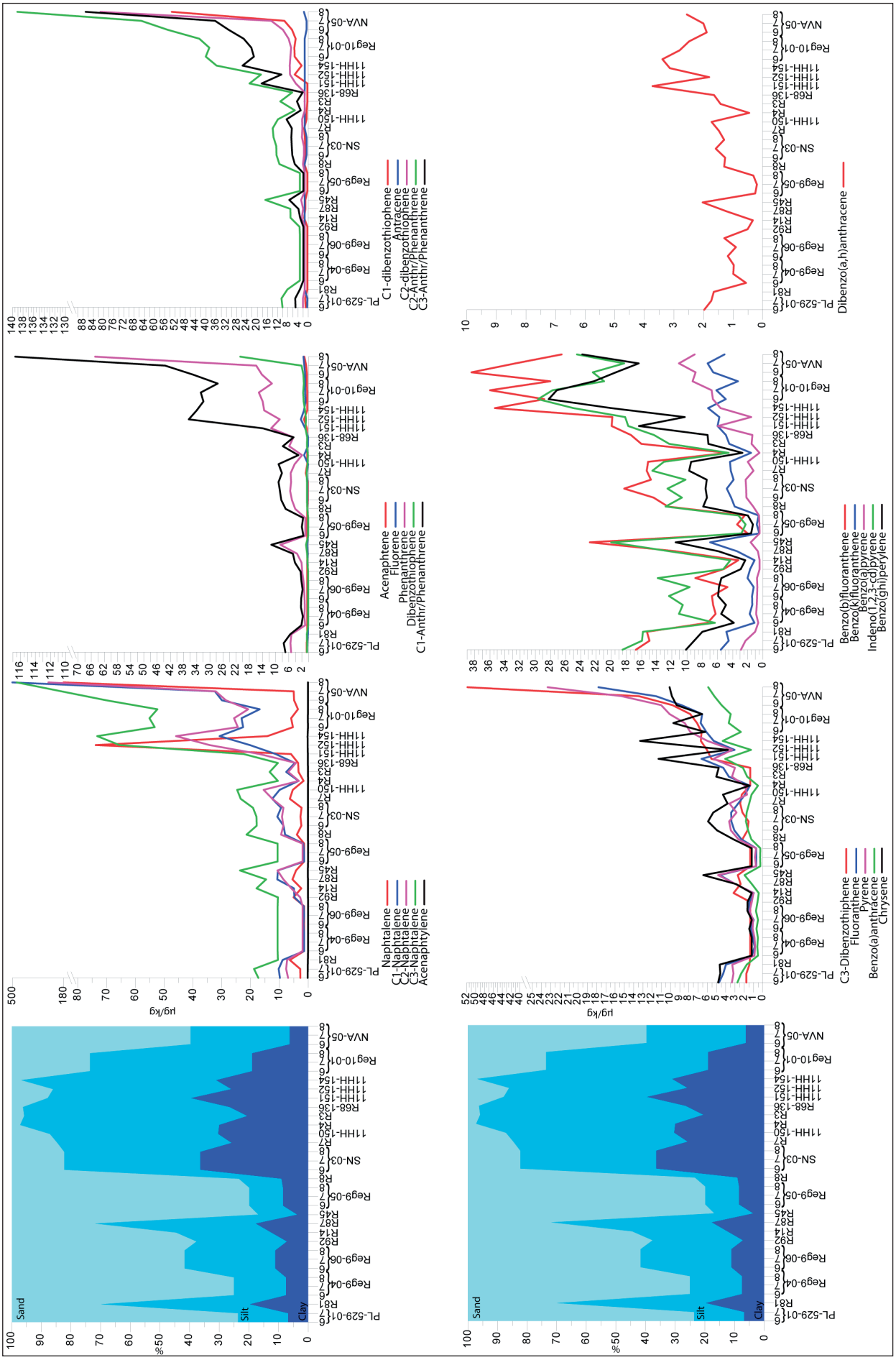

Figure 3. The left panel shows the cumulative grain size for the surface samples. The right panel shows individual PAH concentrations in the different surface sample stations.

For naphthalene, the highest concentrations are at station NVA–05 (replicate NVA05–8) with the lowest at station R4. Apart from station NVA–05, replicate NVA05–08 naphthalene values are <6 µg/kg. It should be noted that NVA05–8 shows significantly higher naphthalene values and also many of the other PAH than the two other replicates (NVA05–6 and NVA05–7) from the same station. Mannvik et al. (2011) published these results and they noticed the significant difference but they did not offer any explanation for it. The difference could be explained, for example, by the patchiness of the sediments; however, this needs further investigation. The acenapthtylene content is highest in sample 154 while acenaphtene is highest at station 152 and lowest at station SN–03. Fluorene is also highest at station 152. Apart from naphthalene, all other PAH concentrations are positively correlated with clay and silt contents.

Phenanthrene is highest at station NVA–05–8 and lowest at station Reg9–05 (replicates Reg9–05–6 and Reg9–05–8). Anthracene is also highest at station NVA–05–8 with lowest concentrations at station PL–529–01–7. The fluoranthene concentration is also highest at station NVA–05–8. It is lowest (below detection limit) at Reg9–05. Similarly, pyrene is highest at NVA–05–8 and lowest at Reg9–05–6 and Reg9–05–8.

The concentration of Benzo(a)anthracene is highest at NVA–05–8 and lowest at Reg9–05–6 and Reg9–05–8. Chrysene is highest at station 154 and lowest (below detection limit) at several stations. Benzo(b)fluoranthene is highest at NVA–05–6 and lowest at Reg9–05–6. Benzo(k)fluoranthene is highest at NVA–05–7 and lowest at Reg9–05–6.

Benzo(a)pyrene is highest at station NVA–05–7 and lowest at Reg9–05–6 (below detection limit) while indeno(1,2,3-cd)pyrene is highest at station Reg10–1–6 and lowest at Reg9–05–7. Benzo(ghi)perylene is lowest in Reg9–05–7 and highest in Reg10–1–6. Dibenzo(a,h) anthracene is highest at station 152 and lowest at Reg9–05–7. Generally speaking, the highest PAH concentrations are associated with the northernmost stations, e.g., NVA–5–08, Reg10 and 154.

Subsurface samples

Concentrations in subsurface samples fluctuate between 35 and 455 µg/kg for SUM PAH, 39–291 µg/kg for NPD, and 26–154 µg/kg for PyrPAH (Table 3; Fig. 4). Multicores 152 and 154 exhibit the highest concentrations of SUM PAH, NPD and PyrPAH. In general, changes in PAH concentrations correlate with grain size, and especially with clay and silt concentration and TOC. Notable high concentrations of SUM PAH, NPD and PyrPAH are seen in the lower part of core 150, corresponding to the time period 1880–1917. In addition, notable changes in NPD are observed in core 152, with a rapid increase observed from 1994 to 2002. There is also a strong increase in NPD content between 2005 and 2009 in core 151 (Average level ~150 µg/kg). Other notable changes include PyrPAH concentrations in core 150 and 151. Both PyrPAH and TOC increase during the mid-1970s in these cores. A similar pattern is observed in cores 152 and 154 during the 1950s and 1930s, respectively.

Results for the individual PAHs in the subsurface samples indicate that the top contributors to PAH composition are Naphthalene, Anthr/Phenanthrene and Benzo(b)floranthene. C3- Naphtalene is the PAH compound with the highest concentration. Individual PAH results are given in Electronic Supplement 2 and Fig. 5. The highest concentrations are recorded for station 154 for nearly every compound. Within core 154, the top five compounds contributing to mean SUM PAH are: C3- Naphtalene (62 µg/kg), C2- Naphtalene (40 µg/kg), C1- Naphtalene (31 µg/kg), C2- Anthr/Phenanthrene (33 µg/kg), and C1- Anthr/Phenanthrene (29 µg/kg). Together, these five compounds contribute 54% (194 µg/kg) to the mean SUM PAH. Within core 150, the top five compounds contributing to mean SUM PAH are: C3- Naphtalene (39 µg/kg), C2- Naphtalene (24 µg/kg), C2- Anthr/Phenanthrene (23 µg/kg), C3- Anthr/Phenanthrene (17 µg/kg), and C1- Anthr/Phenanthrene (16 µg/kg). Together, these compounds contribute 54% (119 µg/kg) to the mean SUM PAH. Within core 151, the top five compounds contributing to mean SUM PAH are: C3- Naphtalene (18 µg/kg), C1- Naphtalene (17 µg/kg), C2- Naphtalene (14 µg/kg), Benzo(b)floranthene (13 µg/kg), and C2- Anthr/Phenanthrene (10 µg/kg). Together, these compounds contribute 51% (72 µg/kg) to the mean SUM PAH. Within core 152, the top five compounds contributing to mean SUM PAH are: C3- Naphtalene (33 µg/kg), C2- Naphtalene (22 µg/kg), C1- Anthr/Phenanthrene (19 µg/kg), C2- Anthr/Phenanthrene (18 µg/kg), and Benzo(b)floranthene (14 µg/kg). Together, these compounds contribute 53% (106 µg/kg) to the mean SUM PAH.

Sources of PAH in surface samples

Fossil Fuel Pollution Index

According to FFPIs, petrogenic PAHs prevailed in surface sediment sample R14 (FFPI = 75%) and three NVA samples (FFPI = 63–89%) (Table 2; Fig. 6). Low FFPI values were found in sediment samples: R81, R68A–135, reg9–04–6, reg9–04–7, reg9–04–8, reg9–05–6, reg9–05–7, reg9–05–8, reg9–06–6, reg9–06–7, and reg9–06–8 (FFPI = 6–39%). This indicates a predominance of pyrogenic PAHs. FFPIs found in other sediment samples suggest a presence of both petrogenic and pyrogenic sources (FFPI = 43.5–60.2). The average FFPI % for all surface samples is 44%.

In subsurface samples, petrogenic PAHs prevailed in the majority of the core samples (FFPI = 61–89%) (Fig. 4). Generally, the petrogenic PAHs start to dominate

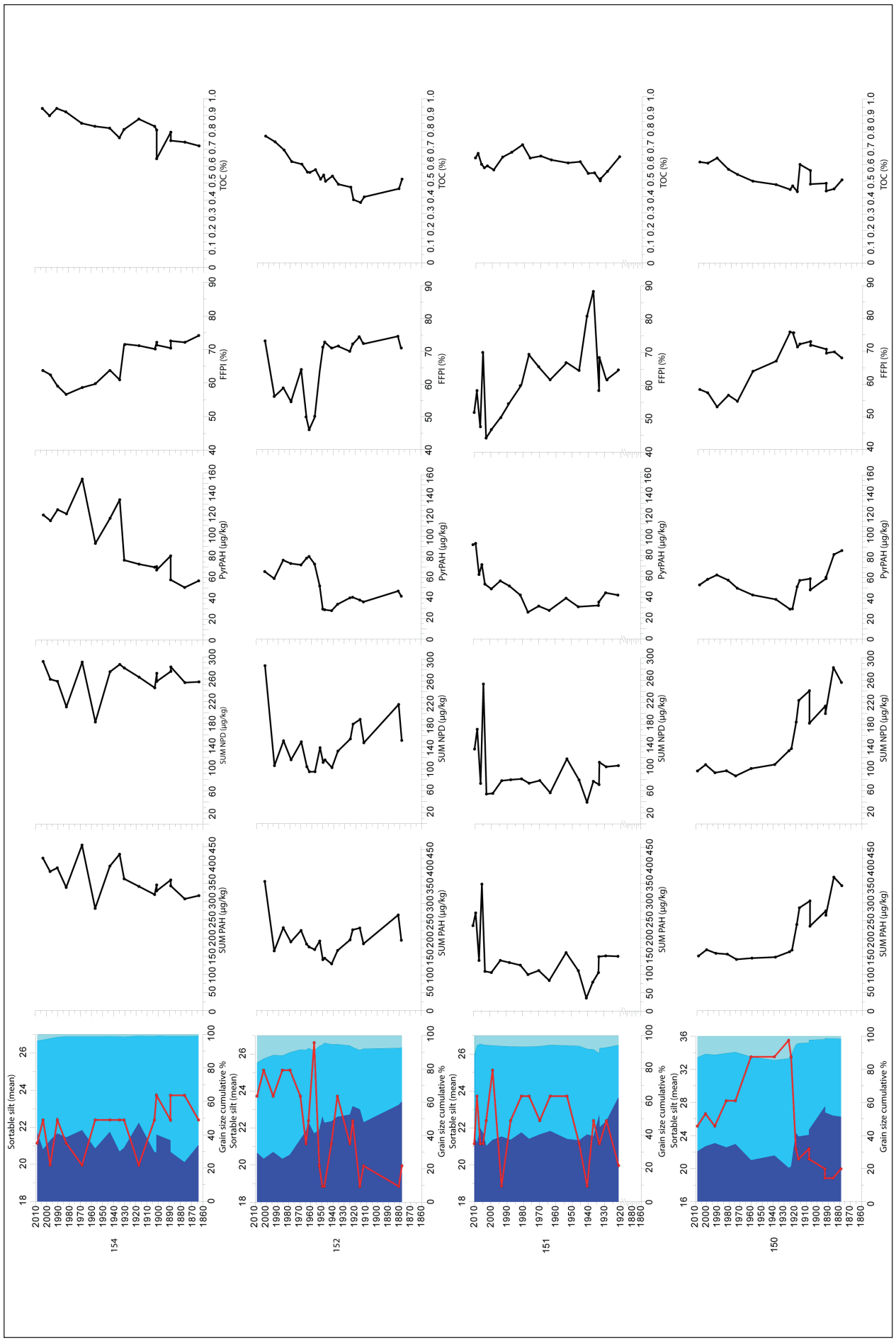

Figure 4. The left panel shows the grain size plotted against calendar years in subsurface samples. Clay, silt and sand contents are indicated with different colors from left to right, respectively, and the red line indicates the sortable silt mean grain size (modified after Junttila et al., 2014). The right panel shows the SUM PAH, SUM NPD, PyrPAH concentrations and FFPI index as well as the TOC content in different calendar years.

Table 3. *FFPI values and selected PAH ratios in surface sediment samples (continued next page).*

Core	*Depth (cm)*	*Age*	*FFPI %*	*SUM PAH µg/kg*	*SUM PAH/ TOC*	*PyrPAH µg/kg*	*PyrPAH/ TOC*	*NPD µg/kg*	*NPD/ TOC*
150	1	2009	58.3	151.9	24.6	53.0	8.6	95.7	15.5
	2	2001	57.3	169.2	27.7	58.4	9.6	107.0	17.5
	3	1993	53.0	159.3	24.8	62.7	9.8	92.5	14.4
	4	1982	56.6	156.9	27.4	57.6	10.1	96.0	16.8
	5	1974	54.8	142.3	26.3	49.7	9.2	86.7	16.0
	6	1960	63.9	145.9	29.2	43.1	8.6	100.1	20.0
	7	1939	67.0	148.6	31.0	38.8	8.1	107.3	22.4
	8	1926	75.9	163.6	36.4	29.2	6.5	132.3	29.5
	9	1924	75.6	168.3	35.7	29.6	6.3	136.2	28.9
	13	1919	71.3	239.5	54.9	51.2	11.7	184.1	42.2
	14	1917	72.2	286.0	47.5	57.3	9.5	223.4	37.1
	15	1907	73.0	305.3	54.0	59.0	10.4	240.9	42.6
	16	1907	72.0	234.9	48.7	48.1	10.0	182.1	37.8
	17	1893	70.6	277.6	57.0	59.1	12.1	213.2	43.8
	18	1893	69.4	265.3	60.3	60.4	13.7	199.6	45.4
	19	1886	69.8	371.5	82.0	82.7	18.2	282.7	62.4
	20	1879	68.0	347.7	68.4	86.5	17.0	255.8	50.4
Average			66.4	219.6	43.3	54.5	10.6	160.9	31.9	75.29
Core	*Depth (cm)*	*Age*	*FFPI %*	*SUM PAH µg/kg*	*SUM PAH/ TOC*	*PyrPAH µg/kg*	*PyrPAH/ TOC*	*NPD µg/kg*	*NPD/ TOC*
151	1	2010	51.9	234.5	37.1	90.4	14.3	135.4	21.4
	2	2009	58.3	269.4	40.9	91.6	13.9	171.2	26.0
	3	2007	47.5	138.8	23.4	61.8	10.4	73.1	12.3
	4	2005	70.2	348.6	60.8	71.3	12.4	253.1	44.2
	5	2003	44.2	108.7	18.6	52.6	9.0	54.0	9.2
	6	1999	47.2	105.5	18.8	48.0	8.6	55.1	9.8
	7	1993	50.8	138.7	21.8	55.7	8.7	78.0	12.2
	8	1988	55.3	132.9	20.0	50.8	7.6	79.8	12.0
	9	1981	60.2	125.7	17.7	42.1	5.9	81.3	11.4
	10	1977	69.3	99.9	15.8	25.7	4.1	73.5	11.6
	11	1970	65.3	110.8	17.2	31.5	4.9	78.3	12.2
	12	1964	61.8	83.5	13.5	27.4	4.4	56.1	9.1
	13	1953	66.9	160.2	26.6	39.1	6.5	117.6	19.5
	14	1946	64.5	110.4	18.1	30.9	5.1	79.3	13.0
	15	1941	80.9	35.2	6.5	n.d.	n.d.	38.9	7.2
	16	1937	88.5	79.0	14.6	n.d.	n.d.	76.9	14.2
	17	1933	58.8	105.4	21.3	32.1	6.5	71.0	14.4
	18	1933	68.5	149.1	29.4	35.4	7.0	111.4	22.0
	19	1929	61.8	151.3	27.5	44.3	8.0	103.2	18.7
	20	1921	64.6	150.1	23.5	42.1	6.6	105.3	16.5
Average			61.8	141.9	23.7	48.5	8.0	94.6	15.8	

Abbreviation: n.d. – not enough data for calculation.

the core samples from 5–9 cm depth to the bottom of the core. Both petrogenic and pyrogenic PAHs (FFPI = 44–60%) were present in the upper part of the core samples. The subsurface samples generally have higher FFPIs than the surface samples.

PAH ratios

Values of PAH ratios: fluoranthene/fluoranthene+pyrene (FLT/FLT+PYR), benzo[a]anthracene/benzo[a]anthracene+chrysene (BAA/BAA+CHR), and phenanthrene/phenanthrene+methyl phenanthrene (PHE/PHE+C1P) are presented in Electronic Supplements 3 and 4. These ratios were applied to provide further insight into the

Table 3. *FFPI values and selected PAH ratios in surface sediment samples (continued from previous page).*

Core	*Depth (cm)*	*Age*	*FFPI %*	*SUM PAH µg/kg*	*SUM PAH/ TOC*	*PyrPAH µg/kg*	*PyrPAH/ TOC*	*NPD µg/kg*	*NPD/ TOC*
152	2	2002	73.2	361.3	46.8	65.8	8.5	287.9	37.3
	3	1994	56.3	167.0	22.7	58.9	8.0	105.7	14.3
	4	1986	58.8	231.8	33.7	76.8	11.2	150.9	22.0
	5	1979	54.6	192.1	31.1	73.6	11.9	116.3	18.9
	6	1969	64.5	224.0	37.3	72.2	12.0	149.1	24.8
	7	1964	49.4	186.0	33.6	78.7	14.2	103.6	18.7
	8	1962	46.1	178.0	32.3	80.5	14.6	94.6	17.2
	9	1957	49.9	170.7	30.1	73.0	12.9	94.6	16.7
	10	1952	64.2	194.5	38.1	51.8	10.2	138.4	27.1
	11	1950	71.1	142.5	26.6	29.2	5.5	111.5	20.8
	12	1948	72.9	146.4	29.5	28.6	5.7	116.1	23.4
	13	1942	70.9	130.6	24.7	27.7	5.2	102.0	19.3
	14	1936	71.7	168.1	35.1	33.9	7.1	132.2	27.6
	15	1925	70.0	197.7	42.9	40.2	8.7	154.4	33.5
	16	1922	72.2	225.9	58.7	40.7	10.6	181.3	47.1
	17	1916	74.5	230.9	62.8	38.0	10.3	190.0	51.6
	18	1913	72.3	186.8	46.5	36.2	9.0	147.3	36.6
	19	1881	74.6	267.5	59.2	46.8	10.3	217.2	48.0
	20	***1878***	***71.1***	***196.7***	***38.6***	***41.7***	***8.2***	***151.6***	***29.7***
Average		65.2	199.9	38.4	52.3	9.7	144.5	28.1	21.4
Core	*Depth (cm)*	*Age*	*FFPI %*	*SUM PAH µg/kg*	*SUM PAH/ TOC*	*PyrPAH µg/kg*	*PyrPAH/ TOC*	*NPD µg/kg*	*NPD/ TOC*
154	2	2003	63.7	418.8	44.5	119.9	12.7	291.4	30.9
	3	1997	62.6	382.2	42.5	114.4	12.7	259.5	28.9
	4	1990	59.2	392.2	41.6	125.0	13.3	255.7	27.1
	5	1982	56.6	338.5	36.7	121.0	13.1	210.0	22.8
	6	1968	58.6	454.6	53.2	154.3	18.1	290.2	34.0
	7	1957	59.7	281.0	33.6	92.6	11.1	182.9	21.9
	8	1943	63.8	397.0	48.1	116.7	14.2	273.0	33.1
	9	1935	61.0	429.5	55.9	134.5	17.5	286.1	37.2
	10	1931	71.6	362.1	44.3	76.6	9.4	279.7	34.2
	11	1917	71.1	341.2	38.8	72.7	8.3	263.2	29.9
	12	1903	70.1	319.0	38.2	69.8	8.4	244.2	29.2
	13	1902	72.1	345.3	42.4	70.4	8.6	270.2	33.2
	14	1902	71.3	329.1	51.1	67.1	10.4	255.8	39.7
	15	1889	70.4	359.0	44.8	80.7	10.1	273.6	34.2
	16	1889	72.5	342.9	45.7	57.8	7.7	281.5	37.5
	17	1876	72.1	307.0	41.4	50.4	6.8	253.5	34.2
	18	1864	74.2	316.0	43.9	56.8	7.9	254.9	35.4
	19	1851	74.5	353.4	49.1	57.7	8.0	288.9	40.1
	20	1839	72.0	347.5	46.5	60.0	8.0	284.1	38.0
Average		67.2	358.8	44.3	89.4	10.9	263.1	32.7	

sources of petroleum PAHs in sediments from this study (Budzinski et al., 1997; Yunker et al., 2002). A graph of FLT/FLT+PYR vs. BAA/BAA+CHR and FLT/FLT+PYR vs. BAA/BAA+CHR PHE/PHE+C1P (Fig. 7) indicates that mixed (petroleum or combustion) sources prevail in most sediment samples. Subsurface samples show similar results to the surface samples (Fig. 8). In addition, the combustion source prevails in surface samples from the cores.

Identification of PAH sources

Contributions of possible sources to total PAH concentration in surface samples were evaluated using source-allocation models (Electronic Supplement 5; Fig. 9).

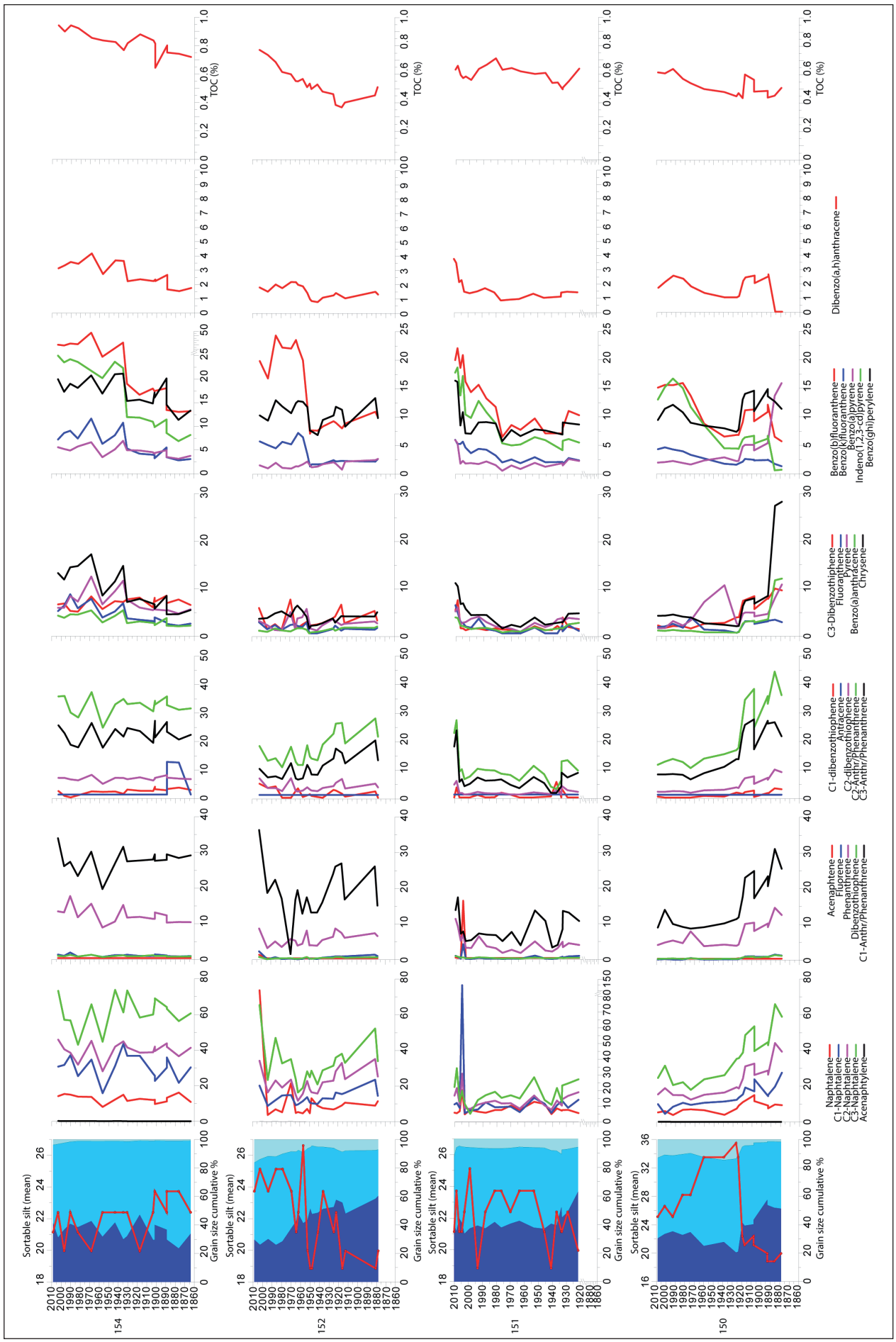

Figure 5. *The left panel shows grain size by calendar year in subsurface samples. Clay, silt and sand contents are indicated with different colors from left to right, respectively. The red line indicates the sortable silt mean grain size (modified after Junttila et al., 2014). The right panel shows the individual PAH concentrations and TOC content by calendar year.*

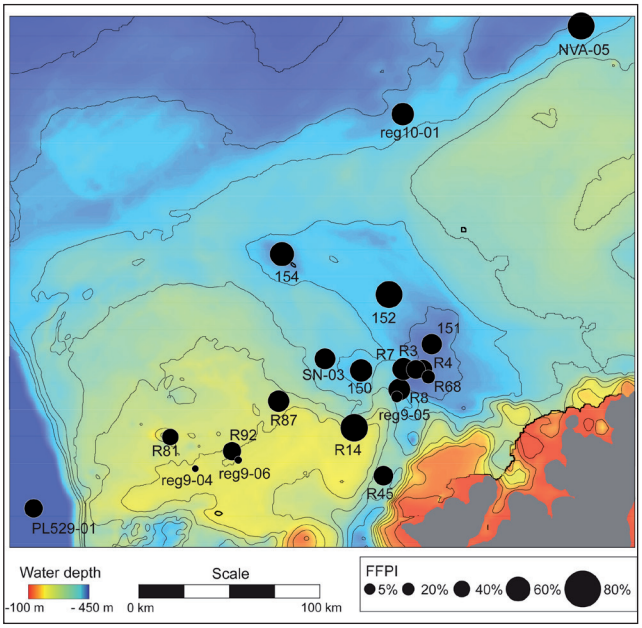

Figure 6. Bathymetric map with FFPI index (%) at surface sample stations.

Based on the results of the source-allocation modeling, pyrogenic PAHs prevailed in 14 of 30 samples (R3, R4, R92, R81, R68A–135, reg9–04–6, reg9–04–7, reg9–04–8, reg9–05–6, reg9–05–7, reg9–05–8, reg9–06–6, reg9–06–7, reg9–06–8) (sum of pyrogenic PAHs 63–100%). In 14 of 30 samples, mixed sources of PAH contamination were identified. Petrogenic PAH predominated in only two of 30 samples (R14 and NVA–05–8) (Table 3). Concentrations of PAH and NPD at station R14 are below average for our dataset while NVA–05–8 has the highest PAH and NPD values measured in this study (Fig. 2).

Discussion

We evaluate patterns of PAHs in surface and subsurface sediments in the Tromsøflaket and Ingøydjupet region of the southwestern Barents Sea. Past and present PAH levels are examined in context with sedimentary properties. We further assess possible contributions from various sources to total PAH concentrations and discuss the role of ocean currents in the transport and deposition of PAH-laden sediments in our study area. These patterns provide baseline information to evaluate the present state of the seafloor environment in relation to increasing petroleum exploration and development in this area.

PAH concentrations

The Norwegian Pollution Control Authorities have developed guidelines for environmental quality of contaminated sediments (Bakke et al., 2010) following the principles of the risk assessment guidelines of the European Water Framework Directive (WFD, 2000). The regulations define five classes based on the ecotoxicity of contaminants including PAHs (Bakke et al., 2010). The five classes are; I: background levels of metal concentrations; II: low concentrations with no toxic effects; III: medium concentrations with toxic effects after chronic exposure; IV: high concentrations with toxic effects after short-time exposure; V: very high concentrations with acute toxic effects.

Almost all SUM PAH and individual PAH concentrations measured in surface sediments collected in this study correspond to background or low levels (level I or level II) after Bakke et al. (2010), following the guidelines of the EU's Water Framework Directive (Electronic

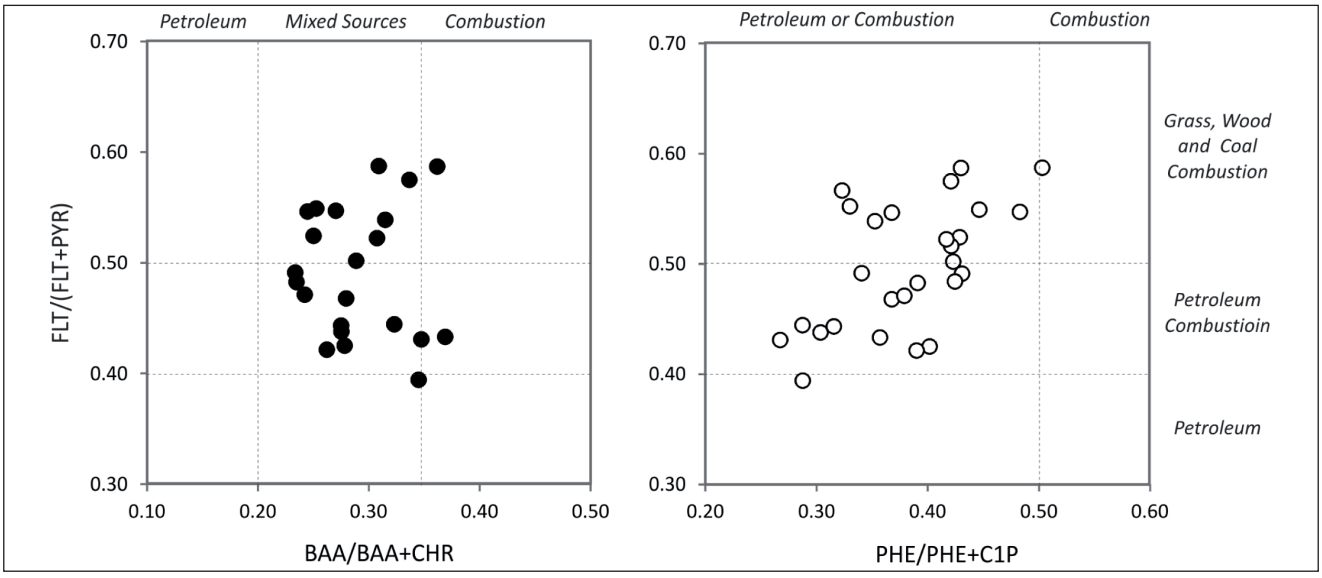

Figure 7. Relationship between PAH ratios and the identification of PAH sources (according to Yunker et al., 2002) in surface sediments.

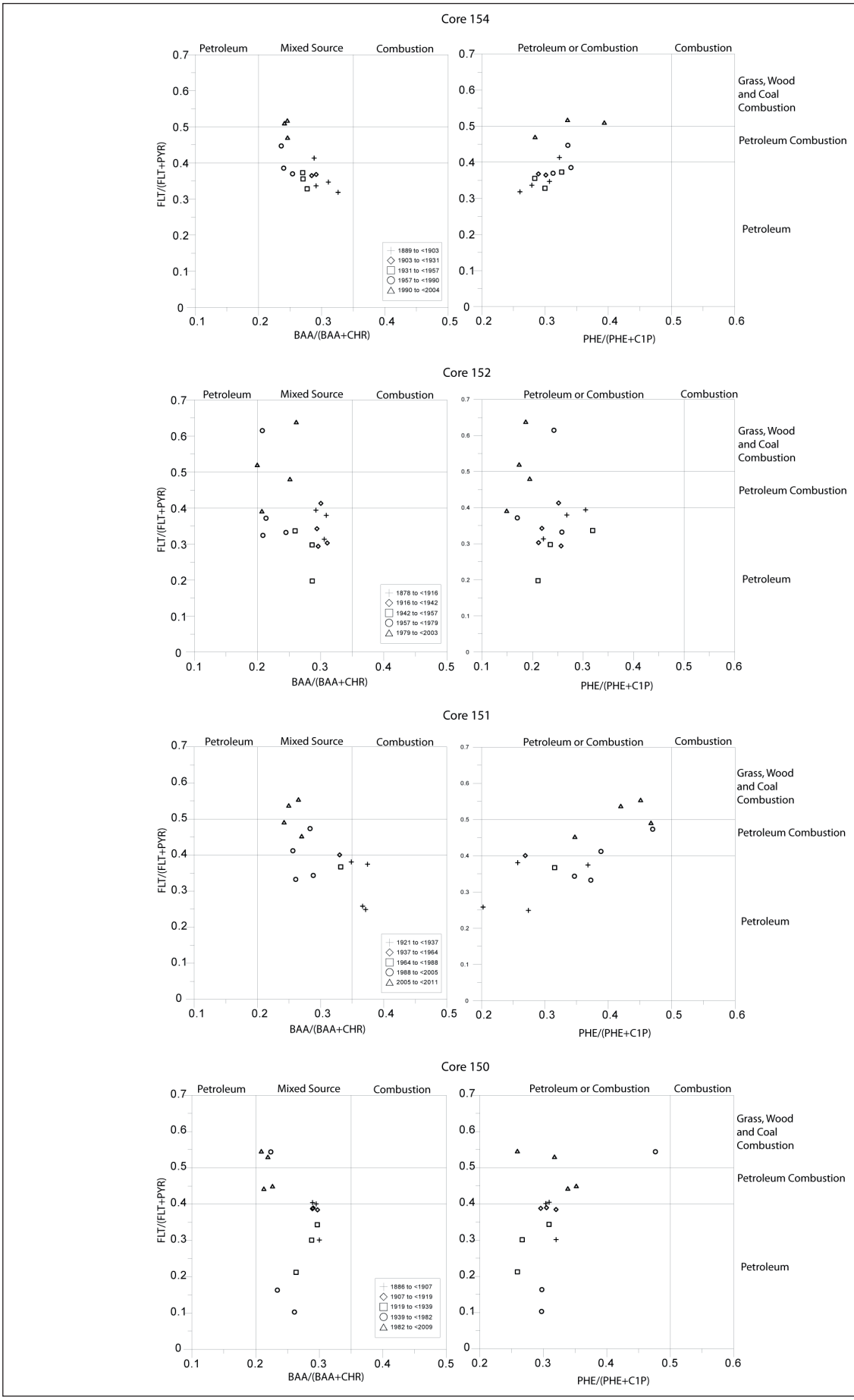

Figure 8. *Relationship between PAH ratios and the identification of PAH sources (according to Yunker et al., 2002) in subsurface sediments.*

Supplement 6; WFD, 2000). Only SUM PAH of station NVA–05–08 has a medium environmental status: level III. (Fig. 2; Electronic Supplement 1).

Similarly, almost all SUM PAH and individual PAH concentrations measured in the downcore sediments correspond to background or low levels (level I or level II). In sediment core 154, the PAH levels (benzo(ghi)perylene) at depth intervals 7–8 cm (~1943) and 8–9 cm (~1935) are medium (level III (Fig. 5)). Taken together, these findings indicate that the low level of petroleum activity carried out in the past decade has not led to any detectable increase in sedimentary PAH concentrations. The levels of SUM PAH and individual PAHs are approximately similar in subsurface and surface samples which further suggests that natural changes have predominated during the past ~150 years. Dahle et al. (2009) also observed only a slight increase in PAH levels in the Southwest Barents Sea compared to datasets from the past two decades.

The predominant compounds in the surface samples (Fig. 2; Table 2) are NPD for the northernmost (Bjørnøyrenna) and Ingøydjupet samples and PyrPAH for the western (shallowest) Tromsøflaket samples. The highest SUM PAH levels were found in Ingøydjupet and in the northernmost samples (Bjørnøyrenna). NPD levels ranged from 16 to 30 µg/kg in Tromsøflaket and from 30 to 291 µg/kg in Ingøydjupet. However, the northernmost stations (Bjørnøyrenna) have the highest contents (>100 µg/kg). The NPD concentration reaches 2046 µg/kg at sample NVA–05. However, this high NPD content was detected in only one of the three replicates. In comparison, Dahle et al. (2009) reported average NPD values of 32 µg/kg in the 1990s (data obtained 1992–1998) and 67 µg/kg in the 2000s (data obtained 2001–2005) for the entire southwestern Barents Sea area. Our average NPD values (Table 2) are 157 µg/kg mainly because of the high values at stations Reg–10 and NVA–05. Without these two stations the average content is 69 µg/kg. This is in line with the level reported by Dahle et al. (2009) for the 2000s.

Similar to NPD, the highest PyrPAH levels in surface sediments are found in Ingøydjupet and Bjørnøyrenna. In western Tromsøflaket, PyrPAH levels are 22–56 µg/kg compared with 10–120 µg/kg in Ingøydjupet (Table 2). The average PyrPAH value in our sample set is 58 µg/kg while Dahle et al. (2009) reported higher average PyrPAH values of 81 µg/kg for the 1990s and 88 µg/kg for the 2000s. For SUM PAH, we report an average of 225 µg/kg which is considerably higher than 129 µg/kg (1990s) and slightly higher than 178 µg/kg (2000s) as reported in Dahle et al. (2009). This high average SUM PAH content (similar to NPD) is caused by high values at stations Reg–10 and NVA–05. Without these two stations the average content is 123 µg/kg, which is more in line with the level reported by Dahle et al. (2009).

As for the surface samples, the predominant compounds in the subsurface are NPD and PyrPAH. The highest concentrations of these compounds were detected in core 154. In this core, NPD levels are 39–291 µm/kg and PyrPAH levels are between 26 and 154 µg/kg (Table 3). These NPD and PyrPAH levels correspond well with the results reported for our surface samples. As no core was collected in the northern Bjørnøyrenna area, we have no subsurface samples to determine whether the high levels of PAH compounds in surface samples from this location extend below the sediment surface.

Generally, the highest individual PAH concentrations are found in the deepest basins (Fig. 1) from which the northernmost site (NVA–05) has the highest concentrations of most of the individual PAHs. Similarly, Dijkstra et al. (2013) observed an increase in heavy-metal contents in surface samples from Ingøydjupet compared to the surface samples from Tromsøflaket. Junttila et al. (2014) hypothesized that the increased sediment accumulation rates at the nearshore stations are the result of the transport of fine sediments from Tromsøflaket mainly by the NCC. These sediments are preferentially deposited northeast of Tromsøflaket in the deeper and calmer areas of Ingøydjupet. Further, Dijkstra et al. (2015) analyzed the metal contents (Ba, Zn, Cr, Hg, Pb, Cd, Cu, Ti) and benthic foraminifera on the same four cores from Ingøydjupet as in this paper. They observed the highest metal concentrations in core 154. The concentrations were attributed to long-distance transport of metals (not a local source) by the NAC. In addition, smectite clay minerals were studied in the same cores. Smectites have a source in the ocean south of the Southwest Barents Sea and therefore further support the suggestion that sediments in Ingøydjupet are the result of long-distance transport of Atlantic water (Vogt & Knies, 2009; Junttila et al., 2010, 2014).

Due to the greater water depths in Ingøydjupet and Bjørnøyrenna, bottom current conditions are relatively calm, thus enabling the settling of fine grained particles which also comprise relatively high contents of TOC. These areas serve as traps for fine-grained sediments which also preferentially absorb particle-reactive compounds such as PAHs (McElroy et al., 1989; Boitsov et al., 2009b). In most of the cores, the majority of the individual PAH concentrations correlate with the amount of clay in individual sediment samples (Fig. 5). Other studies have also reported an increase in PAH as well as heavy-metal concentrations which correlates with an increase in TOC and the fraction of fine-grained material (Boitsov et al., 2009a; Dijkstra et al., 2013, 2015). This supports the idea that PAH concentrations respond to natural variability in the transportation of sediments by bottom currents (Junttila et al., 2014).

However, as a whole, the correlations between SUM PAH, NPD and PyrPAH and grain size in the surface samples are not pronounced (Fig. 2). Water depth serves as the best predictor for these PAH groups at our stations because of the calmer currents as noted earlier (Table 1;

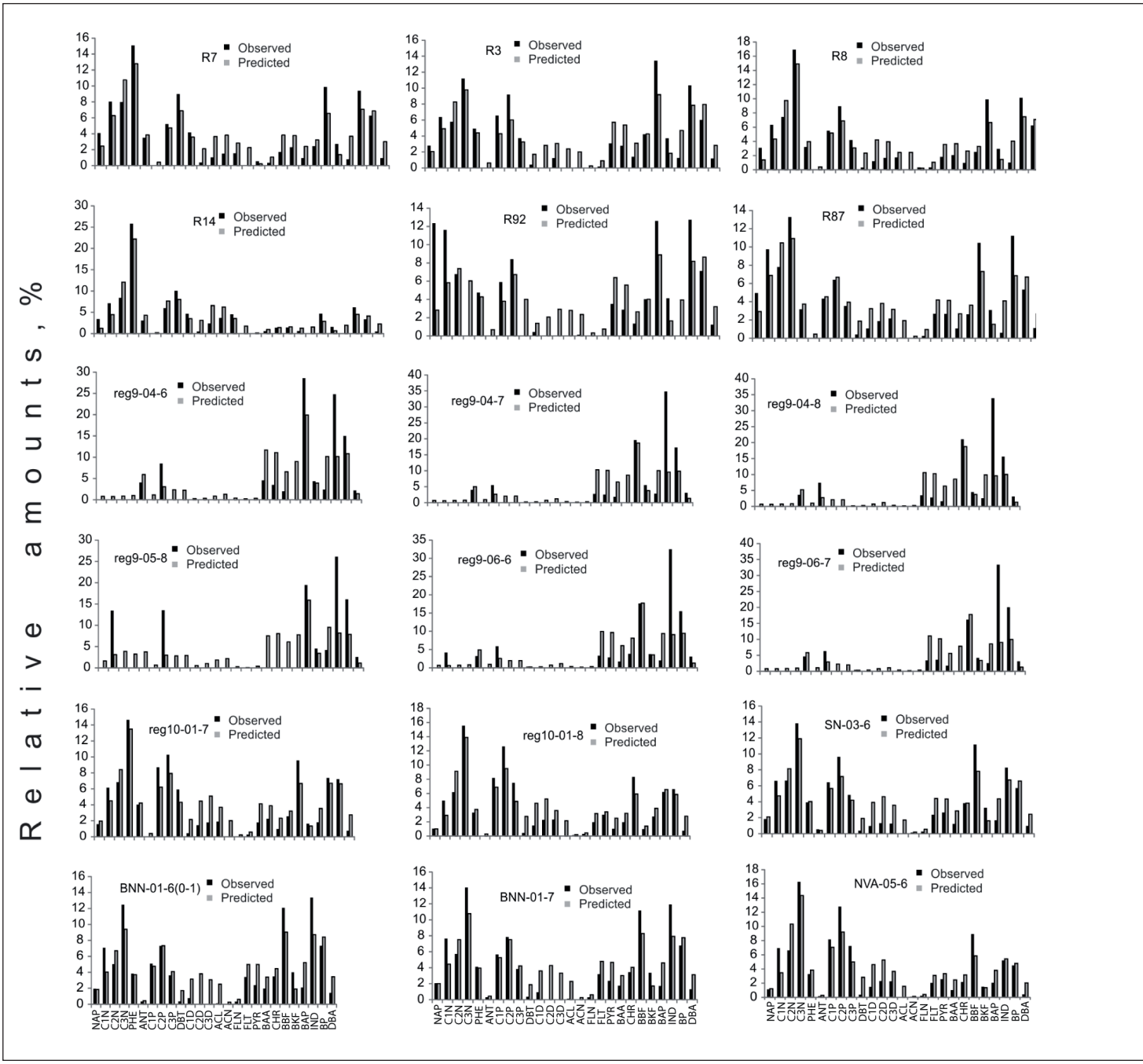

Fig. 1). It should be noted that while the water depths are approximately the same in Ingøydjupet and the northernmost stations of Bjørnøyrenna, the PAH concentrations are higher in Bjørnøyrenna. The reason for this might be Atlantic Water transported by the NAC into Bjørnøyrenna. Atlantic Water is associated with higher TOC contents (Knies & Martinez, 2009) which eventually results in a higher TOC content in the Bjørnøyrenna samples (Dijkstra et al., 2013) which, together with clay particles, contributes to an increased trapping of the contaminants. These results highlight the complex interplay of oceanographic and sedimentary processes that ultimately result in the deposition of higher levels of PAHs in the deep basins of the Southwest Barents Sea where greater water depths, calmer bottom currents, and finer sediments prevail.

These findings extend to the subsurface where we observe a strong positive correlation between PAHs (NPD, SUM PAH), TOC concentration and fine-grained sediments. In core 154, the SUM PAH and NPD levels are relatively stable since 1934, as is grain size. In core 150, SUM PAH, NPD and PyrPAH are correlated with clay concentration. Here, we observe a sudden decrease in concentrations starting from the 1920s and continuing until the 1970s. This pattern is also observed for most metals (Dijkstra et al., 2015), corresponding to a decrease in clay. Overall, Dijkstra et al. (2015) observed a positive

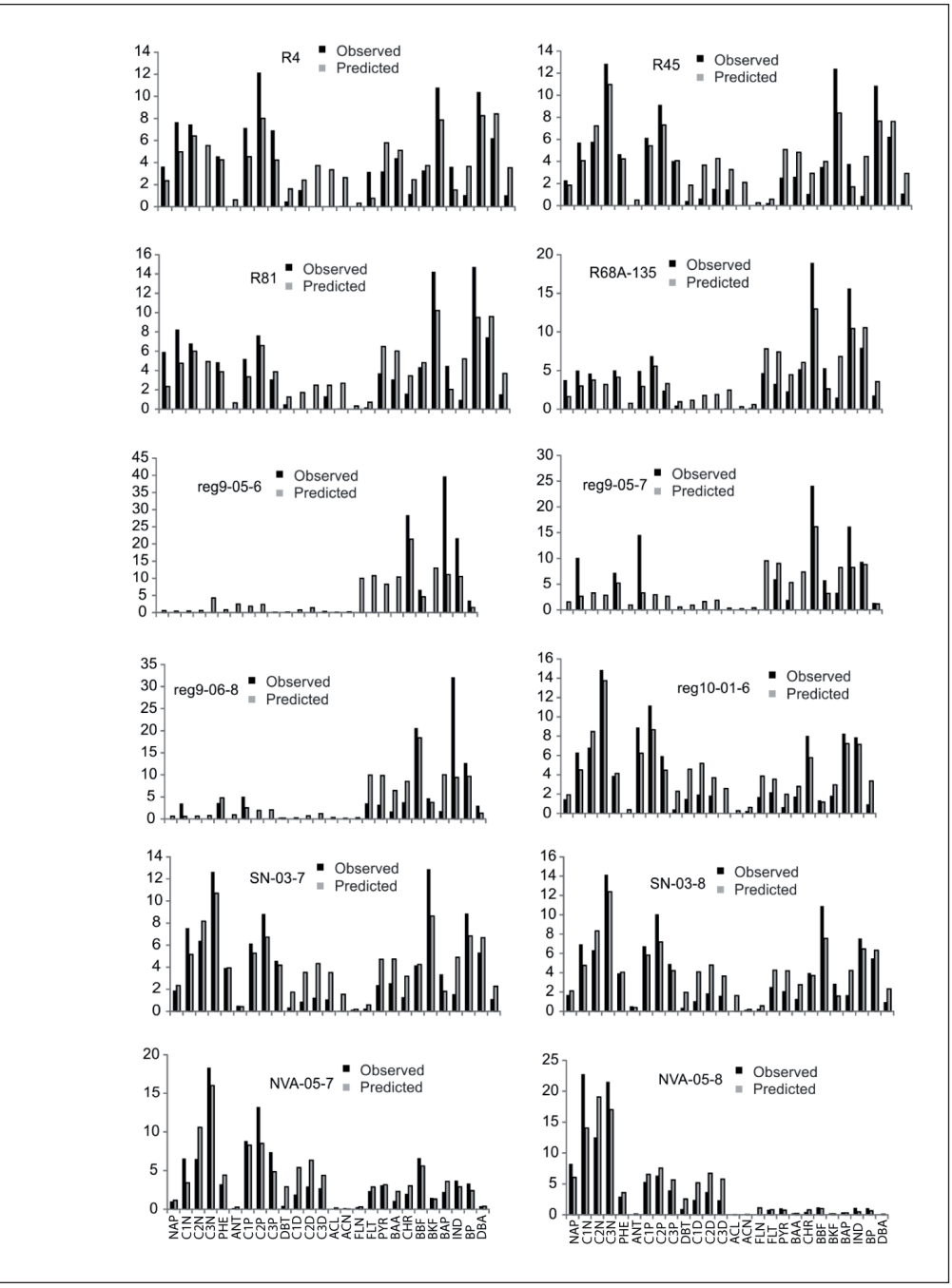

Figure 9. Visualization of the source-allocation modeling for surface samples.
Abbreviations:
NAP – Naphtalene,
C1N – C1-Naphtalene,
C2N – C2-Naphtalene,
C3N – C3-Naphtalene,
PHE – Phenanthrene,
ANT – Anthracene,
C1P – C1-Anthracene/Phenanthrene,
C2P – C2- Anthracene/Phenanthrene,
C3P – C3-Anthracene/Phenanthrene,
DBT – Dibenzothiophene,
C1D – C1-Dibenzothiophene,
C2D – C2-Dibenzothiophene,
C3D – C3-Dibenzothiophene,
ACL – Acenaphthylene,
ACN – Acenaphthene,
FLN – Fluorene,
FLT – Fluoranthene,
PYR – Pyrene,
BAA – Benzo(a)anthracene,
CHR – Chrysene,
BBF – Benzo(b)fluoranthene,
BKF – Benzo(k)fluoranthene,
BAP – Benzo(a)pyrene,
IND – Indeno(1,2,3-cd)pyrene,
BP – Benzo(ghi)perylene,
DBA – Dibenzo(a,h)anthracene.

correlation between metals and either clay or TOC. Generally, PyrPAH correlates better with TOC than the clay fraction as compared to SUM PAH and NPD. In cores 150 and 151 an increase in PyrPAH is noted starting in the mid 1970s and late 1980s, respectively, whereas in cores 152 and 154 the increase started in the 1950s and the 1930s, respectively. These changes show a similarity to the clay and TOC concentrations in cores 150, 151 and 154 and will be further discussed in the chapter on 'Transport mechanism'.

Only a few intervals indicated PAH concentrations that do not correlate to TOC or grain size. In core 152, the NPD and SUM PAH concentrations increase strongly from 1994 to 2002. Also in core 151 a strong increase is observed in both SUM PAH and NPD concentrations in 2005. These trends are also reflected in our profiles for individual PAH concentrations (Fig. 5). Rather than water mass transport and sediment sorting processes, which have been shown to lead to the preferential deposition of fine-grained material with higher PAH concentrations in deeper areas, these patterns suggest a localized source. For NPD and SUM PAH these may be sources of petrogenic and/or anthropogenic origin at these depth intervals. For PyrPAH this might indicate an increase in pyrogenic inputs from natural sources (e.g., forest fires) and/or anthropogenic sources (e.g., wood burning, industry, vehicles). This is discussed further in the next chapter.

Sources of PAH

We apply three different approaches to evaluate source contributions to sediments in this study: FFPI index, source-allocation modeling, and pairwise analysis of selected PAH ratios. The FFPI index approximates the percentage of fossil fuel PAHs relative to total PAHs (Boehm & Farrington, 1984). Source-allocation models are another measure of source contributions. Contributions of the possible source to PAH contamination levels found in sediment samples can be evaluated using non-linear estimation of source-allocation models that finds the linear combination of source PAH profiles that best represents the measured PAH profiles in a given sediment sample (Burns et al., 1997). Here, we also apply the PAH ratios (FLT/FLT+PYR, BAA/BAA+CHR, PHE/PHE+C1P) to provide further insight into the sources of petroleum PAHs in sediments from this study (Budzinski et al., 1997; Yunker et al., 2002). Values of the ratios FLT/FLT+PYR and BAA/BAA+CHR of less than 0.4 and 0.2, respectively, typically indicate petroleum-polluted sediments, while higher values of these two ratios suggest either mixed sources (petroleum or combustion of fossil fuel) or a supply of recent (fresh) organic material (Yunker et al., 2002). Low values of the PHE/PHE+C1P ratio (<0.5) indicate a prevalence of mixed (petroleum or combustion) sources.

Our calculated FFPI values for surface sediment samples indicate a predominance of petrogenic PAHs in these sediments from station R14 (Tromsøflaket) and from the three NVA–05 samples collected in our northernmost sampling area (Table 2; Fig. 6). Low FFPI values, indicating a predominance of pyrogenic PAHs, are mainly associated with sediment samples from Tromsøflaket. At all other stations, the FFPI values suggest the presence of both petrogenic and pyrogenic sources. Dahle et al. (2009) reported an average FFPI value of 21% for 1990 and of 34% for 2000. In this study, our surface samples have an average FFPI value of 44%. Compared to Dahle et al. (2009), our results suggest a doubling in the percentage of fossil fuel PAHs relative to total PAHs over the past ~20 years. This corresponds to a ~1% increase per year since the 1990s, implying an increased emission of fossil fuel.

Our analysis based on source-allocation modeling supports the FFPI findings described above (Table 2; Fig. 9). Atmospheric dust and wood soot are identified as the likely source of pyrogenic PAHs detected at our stations, whereas the likely source of petrogenic PAHs is fresh oil and diesel oil (Electronic Supplement 5). As was seen in the FFPI results, two stations in particular are dominated by petrogenic PAHs, the northernmost stations NVA–05 and R14. Station NVA–05 also exhibits the highest PAH levels found in this study. The NPD value at this station is ten times higher than at other stations. The source-allocation modeling results suggest a combination of fresh oil and diesel oil as the anthropogenic source at this station. At station R14, our modeling indicates diesel oil and lightly weathered diesel oil as the petrogenic source (Electronic Supplement 5).

PAHs linked to fresh oil may be the result of either natural (e.g., natural seeps) or anthropogenic (e.g., offshore production discharges, spillage from vessels) origin sources, or a combination of these two. In the majority of subsurface sediment samples, FFPI values indicate petrogenic PAHs as the dominant source (Table 3; Fig. 4). In general, petrogenic PAHs dominate in sediments deeper than 5–9 cm below the core surface. This indicates a natural origin for the observed petrogenic PAH signature. Both petrogenic and pyrogenic PAHs are found in the upper sediment layers. Based on our core dating, the signal of both petrogenic and pyrogenic PAHs corresponds to a time range of 34–68 years before core collection. Thus, as expected, atmospheric anthropogenic sources are detected in these sediment deposits in the more recent past.

Completing this picture, our pairwise comparison of PAH ratios also indicates that mixed sources (petroleum or combustion) prevail in most of the surface sediment samples (Fig. 7). This pattern is further corroborated for subsurface samples (Fig. 8). In subsurface samples, combustion sources prevail from the ~1980s to the present.

Transport mechanism

The transport and deposition of PAH-laden sediments reflects the combined influence of different water mass transport pathways, their current strengths, sediment properties, such as grain size and TOC content, as well as bottom topography. In the Southwest Barents Sea, it is the interplay between the NCC and the NAC that controls sediment transport (Fig. 1). The NCC, which follows the Norwegian coast towards the north, dominates in the shallow Tromsøflaket, while the offshore and deep-water current NAC is responsible for transporting material northwards along the continental margin. Based on the changes in grain size distributions, Junttila et al. (2014) showed that the NCC is associated with a greater change in the bottom current speed during time than the NAC. The changes in PAH contents in both surface and subsurface sediments of this study correspond mainly with changes in sediment properties, i.e., sediment grain size and TOC.

On the shallow Tromsøflaket where the NCC dominates, sediments are characterized as being relatively low in clay and silt, as a result of high bottom current velocities. Additionally, TOC contents are low, as NAC contains more TOC. In contrast, the NAC dominates along the continental margin and deep-water troughs (e.g., Ingøydjupet and Bjørnøyrenna). These sediment deposits exhibit relatively high clay, silt and TOC contents. This is because of weaker current strength which results in deposition of finer particles and nutrient-rich NAC containing more

TOC than NCC. This leads to higher contents of PAHs in the sediments of NAC-influenced areas because PAHs have a strong affinity for organic matter and therefore tend to accumulate in fine-grained sediments (McElroy et al., 1989). However, even in areas where the NCC dominates, PAH concentrations are higher in deeper waters where fine-grained sediments (clay and silt) are preferentially deposited. The correlation between PAH and clay concentration implies that PAHs are trapped in the fine-grained sediments. This pattern was previously identified by Dijkstra et al. (2013) for heavy metals, with a correlation among fine sediments, heavy-metal concentrations and TOC in this region. Yet a comparison of PAH concentrations in samples from similar water depths collected from two deep basins, Ingøydjupet and the northernmost stations of Bjørnøyrenna, as part of the present investigation, revealed higher SUM PAH concentrations to the north in Bjørnøyrenna. This supports the notion that the NAC is responsible for the long-range transportation of PAH-laden, fine-grained sediments with relatively high TOC contents northwards along the continental margin to the Bjørnøyrenna basin (Knies & Martinez, 2009; Junttila et al., 2014). A similar trend was also noted by Dahle et al. (2006) especially for PyrPAH in NAC waters along a transport path extending from the southwestern Barents Sea towards the southeastern Barents Sea.

The current strength of these water masses also plays a crucial role in determining depositional hot spots for PAH-laden sediments in the Southwest Barents Sea. Junttila et al. (2014) identified decreasing clay concentrations in sediments exposed to increased bottom current strength in an area associated with the NCC. In the present study, there is a good correlation between SUM PAH and clay content in the subsurface samples from core 150 indicating a relationship between SUM PAH and changes in the strength of bottom currents as also suggested by the sortable silt mean grain size (Fig. 3).

Conclusions

The PAH concentrations are at background (level I) to low (level II) levels (Bakke et al., 2010) according to the WFD classification. Only a few samples are of medium level (Level III). SUM PAH, NPD in surface samples are higher than those in the previous studies of Dahle et al. (2009), whereas PyrPAH contents are lower.

Higher levels of PAH are found in Ingøydjupet and Bjørnøyrenna because of greater water depths, finer sediments, higher TOC concentrations, and calmer bottom currents. However, it should be noted that NAC is also one additional contributing transport agent for PAH. NAC transports PAH to the southwestern Barents Sea from farther away, which also contributes to the overall PAH especially in the northern Ingøydjupet and Bjørnøyrenna.

According to source-allocation modeling, most of the PAH in surface samples are of pyrogenic or mixed origin. Pyrogenic PAH consist mainly of atmospheric dust and wood soot input. Two surface samples consist of petrogenic PAH from which R4 in Tromsøflaket is of diesel oil and lightly weathered diesel oil input, and the PAH in NVA–05 in Bjørnøyrenna originates from fresh oil and diesel oil input.

The changes in the PAH contents in surface and subsurface sediments are mainly following the natural changes in sediment grain size and TOC which are controlled by the inflow of AW and the strength of the NAC and NCC.

Acknowledgments. We acknowledge Vladimir Savinov for the source-allocation modeling of the PAH in the surface samples. We also acknowledge the comments of the editor and the two anonymous reviewers. This study was conducted as a part of the Environmental Waste Management (EWMA) project funded by the Research Council of Norway (project nr.195160) and Eni Norway, as well as the Barents Sea Drill Cuttings Research Initiative (BARCUT) project funded by Eni Norway.

References

Andreassen, K., Laberg, J.S. & Vorren, T. 2008: Seafloor geomorphology of the SW Barents Sea and its glaci-dynamic implications. *Geomorphology 97*, 157–177.

Asplin, L., Budgell, P., Ingvaldsen, R., Lien, V., Loeng, H. & Skagseth, Ø. 2006: Comparison of modelled and measured fluxes at the western Barents Slope. *Deliverable D2.6, WP 2, ASOF–N* (31.03.06).

Bakke, S.M., Nøland, S.-A., Møskeland, T., Faksness, L.-G., Gjøs, N. & Oreld, F. 2001: Miljøundersøkelse Statoil/Norsk Hydro, Region IX Finnmark 2000, Hovedrapport 5000–03. *De Norske Veritas rapport 2001–0373*, 51 pp. Available online: http://www.miljodirektoratet.no/old/klif/publikasjoner/offshore/IX/2000IX.pdf.

Bakke, T., Källqvist, T., Ruus, A., Breedveld, G.D. & Hylland, K. 2010: Development of sediment quality criteria in Norway. *Journal of Soils Sediments 10*, 172–178.

Bellec, V.K., Wilson, M., Bøe, R., Rise, L., Thorsnes, T., Buhl-Mortensen, L. & Buhl-Mortensen, P. 2008: Bottom currents interpreted from iceberg ploughmarks revealed by multibeam data at Tromsøflaket, Barents Sea. *Marine Geology 249*, 257–270.

Bjerke, P.L. & Torsethaugen, K. 1989: Environmental conditions on the Norwegian Continental Shelf, Barents Sea. *Norwegian Hydrotechnical Laboratory Report STF60 A89052*, SINTEF, Trondheim.

Bjoroy, M., Hall, P.B., Ferriday, I.L. & Mork, A. 2010: Triassic source rocks of the Barents Sea and Svalbard. *Poster presentation at American Association of Petroleum Geologists convention, 7–10 June 2009, Denver, Colorado*, 8 pp.

Boehm, P.D. & Farrington, J.W. 1984: Aspects of the polycyclic aromatic hydrocarbon geochemistry of recent sediments in the Georges Bank region. *Environmental Science & Technology 18*, 840–845.

Boitsov, S., Jensen, H.K.B. & Klungsøyr, J. 2009a: Natural background and anthropogenic inputs of polycyclic aromatic hydrocarbons (PAH) in sediments of South-Western Barents Sea. *Marine Environmental Research 68*, 236–245.

Boitsov, S., Jensen, H. & Klungsøyr, J. 2009b: Geographical variations in hydrocarbon levels in sediments from Western Barents Sea. *Norwegian Journal of Geology 89*, 91–100.

Boitsov, S., Petrova, V., Jensen, H.K.B., Kursheva, A., Litvinenko, I., Chen, Y. & Klungsøyr, J. 2011: Petroleum-related hydrocarbons in deep and subsurface sediments from South-Western Barents Sea. *Marine Environmental Research 71*, 357–368.

Boitsov, S., Petrova, V., Jensen, H.K.B., Kursheva, A., Litvinenko, I. & Klungsøyr, J. 2013: Sources of polycyclic aromatic hydrocarbons in marine sediments from southern and northern areas of the Norwegian continental shelf. *Marine Environmental Research 87–88*, 73–84.

Budzinski, H., Jones, I., Bellocq, J., Piérard, C. & Garrigues, P. 1997: Evaluation of sediment contamination by polycyclic aromatic hydrocarbons in the Gironde estuary. *Marine Chemistry 58*, 85–97.

Burns, W.A, Mankiewicz, P.J, Bence, A.E, Page, D.S. & Parker, K.R. 1997: A principal-component and least-squares method for allocating polycyclic aromatic hydrocarbons in sediment to multiple sources. *Environmental Toxicology and Chemistry 16*, 1119–1131.

Coakley, J.P. & Syvitski, J.P.M. 1991: Sedigraph technique. *In* Syvitski, J.P.M. (ed.): *Principles, Methods and Application of particle Size Analysis*, Cambridge University Press, Cambridge 368 pp.

Dahle, S., Savinov, V., Petrova, V., Klungsøyr, J., Savinova, T., Batova, G. & Kursheva, A. 2006: Polycyclic aromatic hydrocarbons (PAHs) in Norwegian and Russian Arctic marine sediments: concentrations, geographical distribution and sources. *Norwegian Journal of Geology 86*, 41–50.

Dahle, S., Savinov, V., Klungsøyr, J., Boitsov, S., Plotitsyna, N., Zhilin, A., Savinova, T. & Petrova, V. 2009: Polyaromatic hydrocarbons (PAHs) in the Barents Sea sediments: small changes over the recent 10 years. *Marine Biology Research 5*, 101–108.

Dalsøren, S.B., Endresen, O., Isaksen, I.S.A., Gravir, G. & Sørgård, E. 2007: Environmental impacts of the expected increase in sea transportation, with a particular focus on oil and gas scenarios for Norway and northwest Russia. *Journal of Geophysical Research 112*, D02310.

Dijkstra, N., Junttila, J., Carroll, J., Husum, K., Hald, M., Elvebakk, G. & Godtliebsen, F. 2013: Baseline benthic foraminiferal assemblages and habitat conditions in a sub-Arctic region of increasing petroleum development. *Marine Environmental Research 92*, 178–196.

Dijkstra, N., Junttila, J., Husum, K., Carroll, J. & Hald, M. 2015: Natural variability of benthic foraminiferal assemblages and metal concentrations during the last 150 years in the Ingøydjupet trough, SW Barents Sea. *Marine Micropaleontology* (2015). doi: 10.1016/j.marmicro.2015.09.005

Ersdal, G. 2001: An overview of ocean currents with emphasis on currents on the Norwegian Continental shelf. *Norwegian Petroleum Directorate Preliminary Report, March 2001*, 40 pp.

Gjevik, B. 2000: Summary and assessment of the NDP metocean project. *Project report to the Norwegian Deepwater Project*.

Ingvaldsen, R., Asplin, L. & Loeng, H. 2004: The seasonal cycle in the Atlantic transport to the Barents Sea during the years 1977 – 2001. *Continental Shelf Research 24*, 1015–1032.

Iversen, P.E., Vik Green, A.M., Lind, M.J., Hedegaard Petersen, M.R., Bakke, T., Lichtenthaler, R., Klungsøyr, J., Grafert, T., Natvig, H. & Ersvik, M. 2011: Guidelines for offshore environmental monitoring on the Norwegian continental shelf. *Norwegian Climate and Pollution Agency Report TA 2849/2011*, 49 pp.

Jensen, H.K.B., Knies, J., Finne, T.E. & Thorsnes, T. 2007: Mareano 2006 – Environmental Geochemistry Results from Tromsøflaket, Ingøydjupet, Lopphavet and Sørøysundet. *Norsk geologisk undersøkelse Report 2007.059 (in Norwegian)*, 249 pp. incl. tables and attachments. Available online via www.mareano.no.

Jensen, H.K.B., Knies, J., Finne, T.E. & Thorsnes, T. 2008: Mareano 2007 – miljøgeokjemiske resultater fra Troms II og Troms III. *Norsk geologisk undersøkelse Report 2008.077 (in Norwegian)*, 253 pp. incl. tables and attachments. Available online via www.mareano.no.

Jensen, H.K.B., Boitsov, S., Finne, T.-E., Klungsøyr, J. & Knies, J. 2009: Physical and chemical traces of anthropogenic influence at the seabed and in the sediments in Ingøydjupet, Southern Barents Sea. *Norwegian Journal of Geology 89*, 101–108.

Junttila, J., Aagaard-Sørensen, S., Husum, K. & Hald, M. 2010: Late Glacial–Holocene clay minerals elucidating glacial history in the SW Barents Sea. *Marine Geology 276,* 71–85.

Junttila, J., Carroll, J., Husum, K. & Dijkstra, N. 2014: Sediment transport and deposition in Ingøydjupet, SW Barents Sea. *Continental Shelf Research 76, 53–63*.

Killie, B., Dahle, S., Matishov, G. & dos Santos, J. 1997: Svalbard, Franz Josef Land and eastern Barents Sea contaminations in marine sediments, 1992-1994. *Akvaplan-niva Report 414.96.893,* 50 pp.

Knies, J. & Martinez, P. 2009: Organic matter sedimentation in the western Barents Sea region: Terrestrial and marine contribution based on isotopic composition and organic nitrogen content. *Norwegian Journal of Geology 89*, 79–89.

Mannvik, H.P. & Wasbotten, I.H. 2008: Miljøundersøkelse i Region IX, 2007. *Akvaplan-niva Report 3940.01*. Akvaplan-niva, Tromsø, 118 pp. Available online via http://www.miljodirektoratet.no.

Mannvik, H.P., Wasbotten, I.H. & Cochrane, S. 2011: Miljøundersøkelse i Region IX og X, Barentshavet, 2010. *Akvaplan-niva Report 5000–03. Akvaplan-niva, Tromsø, p. 37. Available online via http://www.miljodirektoratet.no.*

McElroy, A.E., Farrington, J.W. & Teal, J.M. 1989: Bioavailability of polycyclic aromatic hydrocarbons in the aquatic environment. *In* Varanasi, U. (ed.): *Metabolism of Polycyclic Aromatic Hydrocarbons in the Aquatic Environment*, CRC, Boca Raton, FL, USA, pp. 1–40.

Mosby, H. 1968: Surrounding seas. *In* Sømme A. (ed.): *A Geography of Norden,* Cappelens forlag, Oslo, pp. 18–26.

Neff, J.M. 2002: *Bioaccumulation in Marine Organisms*. Elsevier, Oxford, 452 pp.

Neff, J.M., Stout, S.A. & Gunster, D.G. 2005: Ecological risk assessment of PAHs in sediments. Identifying sources and toxicity. *Integrated Environmental Assessment Management 1*, 22–33.

Nøland, S.-A., Fjukmoen, Ø., Petersen, M., Volan, C., Høivang, H., Dokka Torstensen, T.K. & Gaustad, H. 2009: Energy Rapport - Grunnlagsundersøkelser i Region IX og X - Barentshavet, 2008. *Det Norske Veritas hovedrapport 2009-0157 /DNV*, 216 pp. Available online via http://www.miljodirektoratet.no.

Page, D.S., Boehm, P.D., Douglas, G.S., Bence, A.E., Burns, W.A. & Mankiewicz, P.J. 1999: Pyrogenic polycyclic aromatic hydrocarbons in sediments record past human activity: a case study in Prince William Sound, Alaska. *Marine Pollution Bulletin 38*, 247–260.

Sakshaug, E. & Skjoldal, H.R. 1989: Life at the ice edge. *Ambio 18*, 60–67.

Trannum, H.C., Pettersen, A. & Oug, E. 2004: Grunnlagsundersøkelse på Snøhvit og Område C i Barentshavet, 2003. *Akvaplan-niva Report APN-411.2785-1*, Akvaplan-niva, Tromsø, p. 64.

Venkatesan, M.I. 1988: Occurrence and possible sources of perylene in marine sediments – a review. *Marine Chemistry 25*, 1–27.

Vogt, C. & Knies, J. 2009: Sediment pathways in the western Barents Sea inferred from clay mineral assemblages in surface sediments. *Norwegian Journal of Geology 89*, 41–55.

WFD, 2000: Common Implementation Strategy for the Water Framework Directive (2000/60/EC) Guidance Document No. 5. *Transitional and Coastal Waters – Typology, Reference Conditions and Classification Systems*. Produced by Working Group 2.4 – COAST. Office for official publications of the European communities, Luxemburg, p. 116.

Yunker, M.B., Macdonald, R.W., Vingarzan, R., Mitchell, R.H., Goyette, D. & Sylvestre, S. 2002: PAHs in the Fraser River basin: a critical appraisal of PAH ratios as indicators of PAH source and composition. *Organic Geochemistry 33*, 489–515.